

# Chaotic Vibrations of the Duffing System with Fractional Damping

Arkadiusz Syta and Grzegorz Litak

*Faculty of Mechanical Engineering, Lublin University of Technology, Nadbystrzycka 36, PL-20-618 Lublin, Poland*

Stefano Lenci

*Department of Civil and Building Engineering, and Architecture,  
Polytechnic University of Marche, 60131 Ancona, Italy*

Michael Scheffler

*Technische Universität Dresden, Institut für Festkörpermechanik,  
Professur für Dynamik und Mechanismenmechanik 01062 Dresden, Germany*

(Dated: December 26, 2013)

We examined the Duffing system with a fractional damping term. Calculating the basins of attraction, we demonstrate a broad spectrum of non-linear behaviour connected with sensitivity to the initial conditions and chaos. To quantify dynamical response of the system, we propose the statistical 0-1 test as well as the maximal Lyapunov exponent; the application of the latter encounter a few difficulties because of the memory effect due to the fractional derivative. The results are confirmed by bifurcation diagrams, phase portraits and Poincaré sections.

**The concept of fractional derivatives goes back to a discussion that Leibniz and L'Hospital had over 300 years ago about the half order derivative. The problem attracted attention of many scientist (see Podlubny [1] and Petras [2] and references therein). Generally, it is assumed that the fractional order derivative is useful for a better description of real phenomena. For example, damping in mechanical devices is commonly modeled as a function (linear or nonlinear) of first order derivative and can be replaced by fractional damping (in some cases with an appropriate physical meaning). To solve a fractional differential equation, one has to approximate the corresponding derivative operator, which means including information about previous states of the system (the so-called *memory effect*). This effect introduces additional degrees of freedom. Such multidimensional dynamical systems meet difficulties in non-linear analysis and require a special treatment for chaos detection.**

## I. INTRODUCTION

Systems with fractional damping, that depends on the velocity history, have generated a lot of interest and were extensively studied in the last decade [3–9]. Actually, to model complex energy dissipation with a minimum number of parameters using hysteresis and/or memory effect, a fractional order derivative damping term is proposed, namely, the damping force is proportional to a fractional derivative of the displacement, in contrast to the classical case (first order derivative of the displacement). The memory of the system was found to be an important factor in different research areas [7, 8]. For instance, the problem of non-viscous damping with hysteresis has been investigated in the context of applications for a magnetorheological fluid [10]. Similarly, this concept was used to model damping in a vehicle tire [11] and in plates made of composite materials [12, 13]. Furthermore, the memory modelled by fractional derivatives was also ap-

plied to the problem of shock interactions of an impactor with a rigid target [14], to study visco-elastic properties of beams, plates and cylindrical shells [7], to tune of the proportional-integral-derivative (PID) controller and to model heat conduction in complex materials [8]. Finally, fractional derivatives were also used to optimize evolutionary algorithms [8].

Previous researches on the Duffing system with a fractional damping term [5, 6] were focused on the influence of the order of the derivative or amplitude of the excitation on the dynamics of the system. In the present paper, we demonstrate that the system is sensitive to initial conditions, which can be ascertained by determining basins of attraction. Moreover, we quantify different types of attractors by the 0-1 test that can be used instead of the Maximal Lyapunov Exponent (MLE). Contrary to the MLE, the 0-1 test does not need any phase space reconstruction. The main advantage of the test is its fairly low computational effort. It is based on the dynamical system properties of frequency distribution and, like its previous approaches [15, 16], it originates from a single frequency transform.

## II. THE MODEL

We start with the standard well known nonlinear Duffing equation:

$$\frac{d^2x}{dt^2} + \alpha \frac{dx}{dt} - x + x^3 = \delta \cos(\omega t) \quad (1)$$

where  $\alpha \geq 0$  denotes the damping coefficient,  $\delta$  denotes the amplitude and  $\omega$  denotes the frequency of external excitation. The model describes the dynamics of a mass in a double potential well and exhibits chaotic behaviour [17, 18]. To introduce a fractional derivative to the dynamical system, the widely used Grünwald-Letnikov and Riemann-Liouville definitions are applied. Both of them are particular cases of a general fractional order operator - namely, the former represents the  $q$  order derivative, while the later represents the  $q$

fold integral. In this sense, the class of functions described by the Riemman-Liouville definition is broader (function must be integrable) than the one defined by Grünwald and Letnikov (function must be  $m + 1$  continuously differentiable). However, for a function of the Grünwald - Letnikov class, both definitions are equivalent.

Introducing the first order derivative, we will briefly demonstrate the idea of noninteger derivative. Let us consider the first and second order derivative:

$$f'(t) = \lim_{h \rightarrow 0} \frac{f(t) - f(t-h)}{h} \quad (2)$$

$$\begin{aligned} f''(t) &= \lim_{h \rightarrow 0} \frac{f'(t) - f'(t-h)}{h} \\ &= \lim_{h \rightarrow 0} \frac{f(t) - 2f(t-h) + f(t-2h)}{h^2} \end{aligned} \quad (3)$$

Continuing, one can write a general form of the  $n$ -th order derivative:

$$f^n(t) = \lim_{h \rightarrow 0} \frac{1}{h^n} \sum_{j=0}^n (-1)^j \binom{n}{j} f(t-jh) \quad n \in \mathbb{N} \quad (4)$$

which leads to the Grünwald - Letnikov definition [1]:

$$\begin{aligned} \frac{d^q f}{dt^q} &\equiv_a D_t^q f(t) \\ &= \lim_{h \rightarrow 0} \frac{1}{h^q} \sum_{j=0}^{\lfloor \frac{t-a}{h} \rfloor} (-1)^j \binom{q}{j} f(t-jh), \end{aligned} \quad (5)$$

where  $q > 0$  and the binomial coefficients can be extended to real numbers using the Euler Gamma function

$$\binom{q}{j} = \frac{q!}{j!(q-j)!} = \frac{\Gamma(q+1)}{\Gamma(j+1)\Gamma(q-j+1)}; \quad (6)$$

a pair of square brackets  $\lfloor \cdot \rfloor$  appearing in the upper limit of the sum denotes the integer part, while  $a$  is the length of the memory, respectively.

According to the short memory principle [1, 2], the length of system memory can be substantially reduced in the numerical algorithm to get reliable results. Thus, Eq. (5) becomes

$${}_L D_t^q f(t) = \lim_{h \rightarrow 0} \frac{1}{h^q} \sum_{j=0}^{\lfloor N(t) \rfloor} (-1)^j \binom{q}{j} f(t-jh), \quad (7)$$

where  $N(t) = \min(\frac{t-L}{h}, \frac{t}{h})$ . Note that by this choice we do not need initial conditions before  $t = 0$ , as is usually required for other systems with memory. Now, the Duffing system with a fractional damping term has the following form:

$$\frac{d^2 x}{dt^2} + \alpha \frac{d^q x}{dt^q} - x + x^3 = \delta \cos(\omega t) \quad (8)$$

Equation (8) can be decomposed into a set of equations of lower degree:

$$\begin{aligned} {}_L D_t^1 x(t) &= y(t) \\ {}_L D_t^q x(t) &= w(t) \\ {}_L D_t^1 y(t) &= x(t) + \alpha w(t) - x^3(t) + \delta \cos(\omega t) \end{aligned} \quad (9)$$

The set of equations can be written in the discretized form by the following fractional order Newton-Leipnik algorithm [2]:

$$x(t_k) = x(t_{k-1}) + y(t_{k-1})h \quad (10)$$

$$x(t_k) = w(t_{k-1})h^q - \sum_{j=1}^{N-1} c_j^{(q)} x(t_{k-j}) \quad (11)$$

$$\begin{aligned} y(t_k) &= y(t_{k-1}) + [\alpha w(t_{k-1}) - x^3(t_{k-1}) \\ &\quad + \delta \cos(\omega(t_{k-1}))]h, \end{aligned} \quad (12)$$

where  $h$  is the integration step and the coefficients  $c_j^{(q)}$  satisfy the following recursive relations:

$$c_0^{(q)} = 1, \quad c_j^{(q)} = \left(1 - \frac{1+q}{j}\right) c_{j-1}^{(q)}. \quad (13)$$

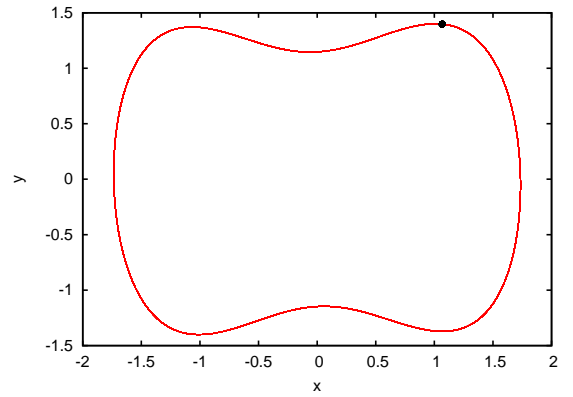


FIG. 1. The phase portraits and Poincaré point for the period one numerical solution of Eqs. (10) - (12) with  $q = 0.6$ ,  $\alpha = 0.15$ ,  $\delta = 0.3$  and  $\omega = 1.0$  for the initial conditions  $(x_0, y_0) = (0.2, 0.3)$ .

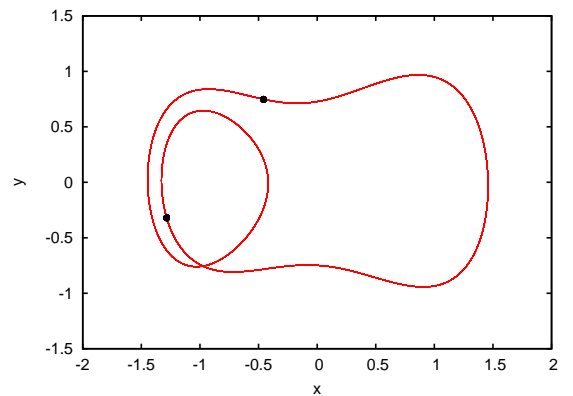


FIG. 2. The phase portraits and Poincaré sections for the period two numerical solution of Eqs. (10) - (12) with  $q = 0.8$ ,  $\alpha = 0.15$ ,  $\delta = 0.3$  and  $\omega = 1.0$  for the initial conditions  $(x_0, y_0) = (0.2, 0.3)$ .

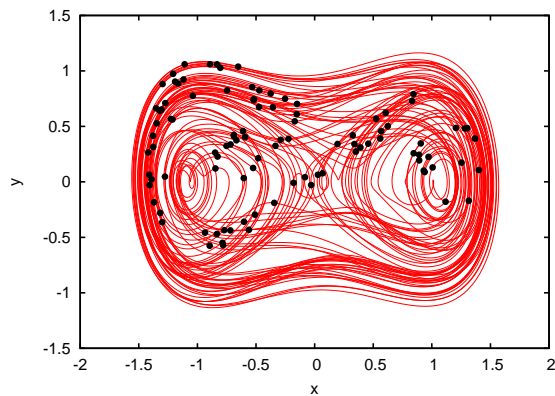


FIG. 3. The phase portraits and Poincaré sections for the chaotic numerical solution of Eqs. (10-12) with  $q = 1.0$ ,  $\alpha = 0.15$ ,  $\delta = 0.3$  and  $\omega = 1.0$  for the initial conditions  $(x_0, y_0) = (0.2, 0.3)$ .

Note that by comparing the left hand sides of Eqs. 10 and 11 we get the formula:

$$w(t_{k-1}) = \frac{1}{h^q} [x(t_{k-1}) + y(t_{k-1})h + \sum_{j=1}^{N-1} c_j^{(q)} x(t_{k-j})] \quad (14)$$

which can be used in Eq. (12).

The set of equations Eqs. (10-12) has been solved numerically for the system parameters  $\alpha = 0.15$ ,  $\delta = 0.3$ ,  $\omega = 1.0$  and with initial conditions  $(x_0, y_0) = (0.2, 0.3)$ . The phase portraits for the order of the derivative  $q = 0.6, 0.8, 1.0$  (the integration step was  $h = \pi/100$ ) are plotted in Figs. 1 - 3, respectively.

Analyzing Figs. 1 - 3, one can notice the evolution of the solution with increasing  $q$ : from period one to period two behaviour through a period doubling bifurcation, to non-periodic (chaotic) solution. Note that for  $q = 1.0$  the coefficients  $c_j = 0$ ,  $j = 1, \dots, n$  (Eq. 13) and we get the standard double-well Duffing model without the memory effect.

### III. BIFURCATIONS CAUSED BY THE ORDER OF THE DERIVATIVE

A more systematic analysis of the system behaviour and of its evolution by changing the order of the derivative  $q$  can be performed by using a corresponding bifurcation diagram. In Fig. 4 one can clearly see the regions of  $q$  for which the system response changes from non-periodic to periodic through a period doubling cascade, and again to non-periodic (for the same initial condition  $(x_0, y_0) = (0.2, 0.3)$ ). Note that for  $q = 1$  we get a non-periodic solution corresponding to the solution for the standard Duffing model with a viscous damping term.

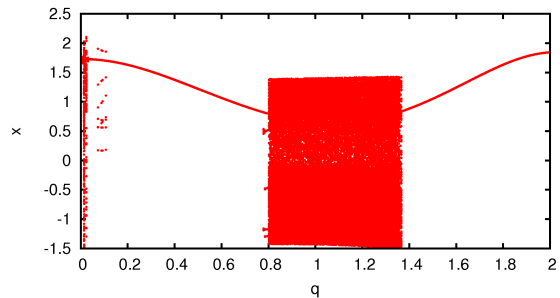


FIG. 4. The bifurcation diagram of the  $x$  coordinate versus the order of the derivative  $q \in [0.01, 2.0]$ ;  $\Delta q = 0.001$  and initial conditions for each  $q$  were  $(x_0, y_0) = (0.2, 0.3)$ . Other system parameters are:  $\alpha = 0.15$ ,  $\delta = 0.3$ , and  $\omega = 1.0$ .

### IV. TEST 0-1 FOR PERIODIC AND NONPERIODIC SOLUTIONS

To quantify the results obtained, we use the 0-1 test for chaos detection [19–26]. This test combines both spectral and statistical properties of the system and can distinguish different types of dynamic of the system by computing a number  $K \in \{0, 1\}$ .

Below, a brief description of the test 0-1 is reported. First of all, we change the coordinates from  $(x, \dot{x})$  to a new set  $(p, q)$  defined as follows

$$p(n) = \sum_{j=1}^n \tilde{x}_j \cos(jc), \quad q(n) = \sum_{j=1}^n \tilde{x}_j \sin(jc), \quad (15)$$

where  $\tilde{x} = [\tilde{x}_1, \tilde{x}_2, \tilde{x}_3, \dots]$  is the discrete time series sampled from the originally simulated  $x$  using one-fourth of excitation period (as in [27]). The time interval  $T/4$  ( $T = 2\pi/\omega$ ) corresponds to the nodal autocorrelation function of excitation harmonic term  $\delta \cos(\omega t)$ . Note that, relevant sampling can make shorter the length of time series used in the calculations, thus leading to a reduction in the computation time. Finally,  $c$  is constant,  $c \in (0, \pi)$ . One can see that Eq. (15) resembles the Fourier transform for a chosen frequency (in the limit of larger  $n$ ).

In the next step, one computes the Mean Square Displacement (MSD) of  $p$  and  $q$ :

$$\text{MSD}(c, j) = \frac{1}{n-j} \sum_{i=1}^{n-j} \{ [p(i+j) - p(i)]^2 + [q(i+j) - q(i)]^2 \}, \quad (16)$$

where  $0 \ll j \ll n$  (in practice  $n/100 \leq j \leq n/10$ ). The main criterion is based on the trends of  $\text{MSD}(c, j)$  in the higher  $j$  limit. It is bounded for regular dynamics or unbounded for chaotic dynamics [19–26].

The final quantity  $K$  is calculated as an asymptotic growth rate of MSD (here given by the correlation method):

$$K(c) = \frac{\text{Cov}[j, \text{MSD}(c, j)]}{\sqrt{\text{Cov}[j, j] \cdot \text{Cov}[\text{MSD}(c, j), \text{MSD}(c, j)]}}, \quad (17)$$

where  $j$  is based on a series of natural numbers:  $j = n/100, n/100 + 1, \dots, n/10$ , and  $\text{Cov}[x, y]$  denotes the corresponding covariance of two series where for the same arguments  $x = y$  we get variance, while for a different ( $x = j$  and  $y = \text{MSD}(c, j)$ ) it can be expressed as the expectation value  $E[\cdot]$ :

$$\begin{aligned} \text{Cov}[j, \text{MSD}(c, j)] &= \\ E[(j - E[j]) \cdot (\text{MSD}(c, j) - E[\text{MSD}(c, j)])]. \end{aligned} \quad (18)$$

Unfortunately, the final value  $K$  might differ for different values of  $c$ , so we took 100 values of  $c$  equally spaced from the interval  $(0.1, \pi - 0.1)$  and computed  $K$  as the median. An example of the function  $K(q)$  obtained with this algorithm is reported in Fig. 5.

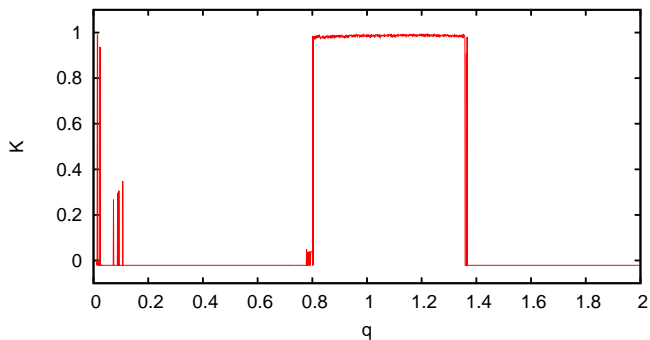


FIG. 5.  $K$  versus  $q$  with the sampling  $\Delta q = 0.001$ , the initial conditions for each  $q$  were:  $(x_0, y_0) = (0.2, 0.3)$ . Other system parameters:  $\alpha = 0.15$ ,  $\delta = 0.3$ , and  $\omega = 1.0$ .

From both Fig. 4 and Fig. 5, one can observe regions corresponding to the regular motion ( $K \approx 0$  for  $q \in [0.1, 0.8] \cup [1.45, 2]$ ) and regions corresponding to the chaotic motion ( $K \approx 1$ , for  $q \in (0.8, 1.45)$ ).

## V. MAXIMAL LYAPUNOV EXPONENT

We have also estimated the MLE, which is commonly used to describe the type of the dynamical systems response. In our system this number has no direct meaning as the system dimension could be undetermined. That is why one cannot use the standard Wolf algorithm with the Jacobi matrix [28], nor the Kantz algorithm with a phase space embedded from a time series [29]. Instead, we measured the distance  $d(i)$  between reference and test orbits, starting from disturbed initial conditions with some arbitrary small initial distance  $d_0(i)$ ,

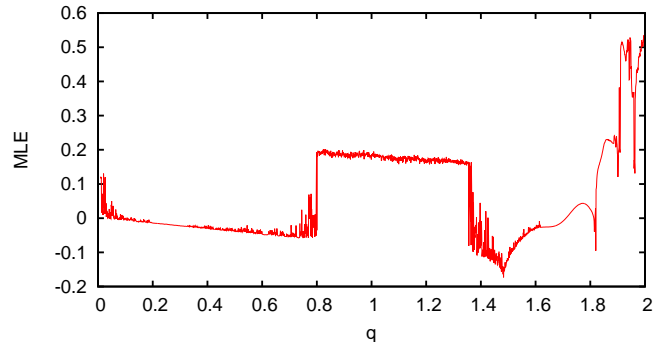


FIG. 6. Maximal Lyapunov Exponent as a function of the fractional order  $q \in [0.01, 2.0]$  and  $\Delta q = 0.001$ . The distance between neighbouring trajectories has been estimated in one tenth of the excitation period interval  $T$  ( $T = 2\pi/\omega$ ). Other system parameters:  $\alpha = 0.15$ ,  $\delta = 0.3$ , and  $\omega = 1.0$ .

$i = 1, \dots, N$ , where  $i$  denotes the subsequent interval which is fairly smaller with respect to the excitation period. Finally, the approximated exponent can be estimated via the following summation

$$\text{MLE} = \frac{1}{\Delta t} \sum_{i=1}^N \ln(d/d_0), \quad (19)$$

where the time interval is  $\Delta t = 2\pi/(100\omega)$  and  $N$  is sufficiently large.

Note that the dimensionality of the examined system with fractional damping could increase; here, for simplicity, the MLE was estimated in a two-dimensional phase space  $(x, \dot{x})$ .

Figure 6 shows variations of the MLE with respect to the parameter  $q$ .

Analyzing the MLE results, one can observe fairly good agreement with the 0-1 test results in the interval of  $q \in [0, 1.5]$ . Beyond the value  $q = 1.5$ , the MLE is inconsistent with the bifurcation diagram and 0-1 test results. This discrepancy corresponds to the lack of information about the distance in higher dimensions in the algorithm given by Eq. 19.

## VI. BASINS OF ATTRACTION

In the previous section, we estimated the MLE testing sensitivity of solutions to perturbations along the trajectory for given initial conditions. However, the global dynamical properties of our Duffing model with fractional damping, showing a variety of solutions, can be investigated by basins of attractions. The stability of particular solutions can be measured by the size of corresponding basins of attraction. We estimated such basins for our system for three selected values of derivative order of the damping term:  $q = \{0.6, 0.8, 1.0\}$  and the range of initial conditions  $(x_0, y_0) \in [-5, 5] \times [-10, 10]$ .



FIG. 7. Basins of attraction for  $q = 0.6$ , and  $\alpha = 0.15$ ,  $\delta = 0.3$ ,  $\omega = 1.0$ . The uniform colour covering the whole region of initial conditions corresponds to the global period one regular solution.

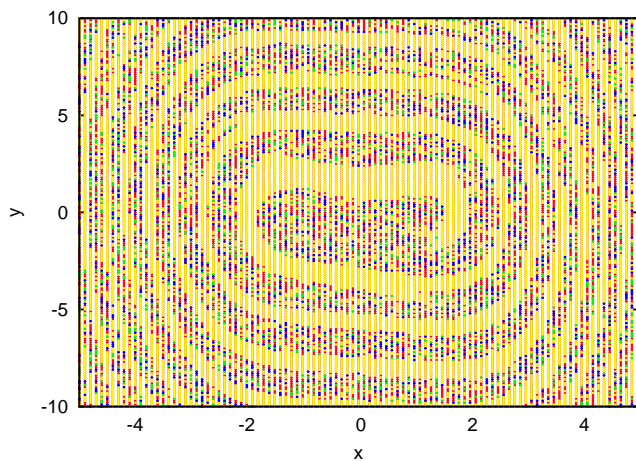


FIG. 8. Basins of attraction for  $q = 0.8$  and  $\alpha = 0.15$ ,  $\delta = 0.3$ ,  $\omega = 1.0$ . Note the colours denote the interplay of four different solutions. Yellow - denotes the period one regular solution; green and blue - two different period two solutions; red - non-periodic (chaotic) solution.

Based on Figs. 7 - 9 one can compare the complexity of solutions with respect to initial conditions and the particular attractors distributions calculated for corresponding steady state solutions.

Figures 7 - 9 show significantly different dynamical behaviour: for  $q = 0.6$  there is only one attractor that corresponds to the period one solution (Fig. 1), for  $q = 0.8$  there are four types of attractors: period one, period 2 type a (Fig. 2), period 2 type b and non-periodic, for  $q = 1.0$  there are two types of attractors: period one and non-periodic (fig. 3). Moreover, comparing figures 8 and 9, one can observe very similar regions of initial conditions corresponding to the periodic solution (yellow) mixed with regions corresponding to different solutions: period two (green, blue - fig. 8) and non-periodic (red).

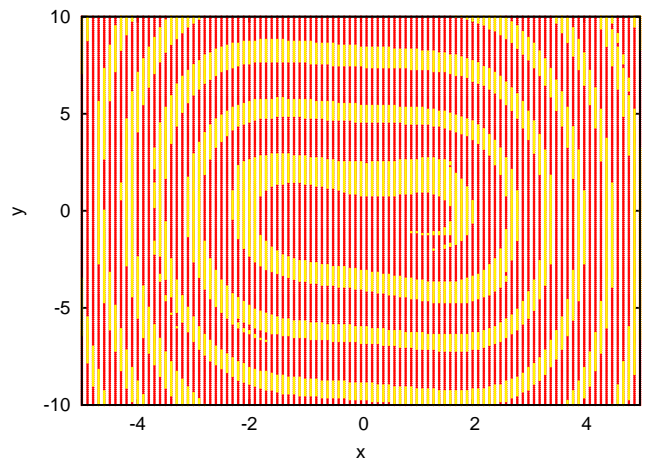


FIG. 9. Basins of attraction for  $q = 1.0$  and  $\alpha = 0.15$ ,  $\delta = 0.3$ ,  $\omega = 1.0$ . Note that colours denote different solutions. Yellow - denotes the period one regular solution while red - non-periodic (chaotic) solution.

In Fig. (8) three different regions involving points belonging to the boundaries of two other basins define Wada basins [30, 31]. In this case the dynamics of the system becomes even more unpredictable than these of fractal border separating two regions.

## VII. CONCLUSIONS

In the paper, we examined the dynamics of the Duffing model with a fractional damping term. Using nonlinear methods (phase diagrams, Poincaré sections and bifurcation diagrams), we highlighted significantly different system responses by varying the order of the derivative (from non-integer to integer). We also quantified the type of motion by the values of two indicators: 0-1 test which is based on statistical properties of phase coordinate, and the approximate maximal Lyapunov exponent which is based on geometrical properties of attractor in phase space. The fractional order of damping introduces memory effects that extend the dimension of the phase space. As a consequence of an uncertainty in the dynamical system dimension, the maximal Lyapunov exponent values may not correspond to the properties of the attractor. In that case, the 0-1 method appeared to give more adequate results. We also found sensitivity to initial condition in the considered system. Interestingly, different values of the order of damping change dramatically the basins of attraction: from one attractor (periodic) to four attractors (periodic, two different period two solutions and non-periodic) exhibiting Wada basins, and finally, to two attractors (period one and non-periodic).

One should note that any system with a fractional derivative is characterized by long transient intervals appearing before reaching the stationary state. This property complicates the investigation of the system dynamics. We would like to stress that our results for dynamics of the system were obtained after

cutting off the corresponding long transients.

Agreement No. 245479, and of the Polish National Science Center (GL & AS) under grant No. 2012/05/B/ST8/00080.

#### ACKNOWLEDGMENT

The authors gratefully acknowledge the support of the 7th Framework Programme FP7- REGPOT-2009-1, under Grant

- 
- [1] I. Podlubny, *Fractional Differential Equations*. San Diego: Academic Press, 1999.
- [2] I. Petras, *Fractional-Order Nonlinear Systems: Modeling, Analysis and Simulation*. New York: Springer, 2010.
- [3] J. Padovan and J. T. Sawicki, *Nonlinear Dynamics* 16, 321 (1998).
- [4] M. Seredynska and A. Hanyga, *Acta Mechanica* 176, 169 (2005).
- [5] X. Gao and J. Yu, *Chaos Solitons Fractals* 24, 1097 (2005).
- [6] L.J. Sheu, H.K. Chen, and L.M. Tam, *Chaos Solitons Fractals* 32, 1459 (2007).
- [7] Y.A. Rossikhin and M.V. Shitikova, *App. Mech. Rev.* 63, 010801 (2010).
- [8] J.A.T. Machado, M.F. Silva, R.S. Barbosa, I.S. Jesus, C.M. Reis, M.G. Marcos, A.F. Galhano, *Mathem. Prob. Engineering* 639801 (2010).
- [9] R.E. Mikens, K.O. Oyediji, and S.A. Rucker, *Journal of Sound and Vibration* 268, 842 (2003).
- [10] A. Rodriguez and N. Iwata and F. Ikhoulane and J. Rodellar, *Smart Materials and Structures* 18, 015010 (2009).
- [11] B.G. Kao, *Tire Science and Technology* 28, 72 (2000).
- [12] P.-Y. Kuo, S.-Y. Wang, J.H. Chen, H.-C. Hsueh, and M.J. Tsai, *Materials and Design* 30, 3489 (2009).
- [13] S. Mueller, M. Kaestner, J. Brummund, and V. Ulbricht, *Comput. Mech.* 51, 999 (2013).
- [14] T.M. Atanackovic and D.T. Spasic, *ASME Journal of Applied Mechanics* 71, 134 (2004).
- [15] A.S. Pikovsky, M.A. Zaks, U. Feudel, and J. Kurths, *Phys. Rev. E* 52, 285 (1995).
- [16] T. Yalcinkaya and Y.-C. Lai, *Phys. Rev. E* 56, 1623 (1997).
- [17] F.C. Moon and P.J. Holmes, *Journal of Sound and Vibration*, 65, 275 (1979).
- [18] J. Guckenheimer and P. Holmes, *Nonlinear Oscillations, Dynamical Systems, and Bifurcations of Vector Fields*: Springer-Verlag, 1983.
- [19] G.A. Gottwald and I. Melbourne, *Proceedings of the Royal Society A* 460, 603 (2004).
- [20] G.A. Gottwald and I. Melbourne, *Physica D* 212, 100 (2005).
- [21] I. Falconer, G.A. Gottwald, I. Melbourne, K. Wormnes, *SIAM J. App. Dyn. Syst.* 6, 395 (2007).
- [22] G. Litak and A. Syta and M. Wiercigroch, *Chaos, Solitons and Fractals* 40, 2095 (2009).
- [23] B. Krese and E. Govekar, *Nonlinear. Dyn.* 67, 2101 (2012).
- [24] G. Litak, S. Schubert, and G. Radons, *Nonlinear. Dyn.* 69, 1255 (2012).
- [25] G. Litak, A. Syta, M. Budhraj, and L.M. Saha, *Chaos, Solitons & Fractals* 42, 1511 (2009).
- [26] G. Litak, D. Bernardini, A. Syta, G. Rega, A. Rysak, *Eur. Phys. J. Special Topics* 222, 1637 (2013).
- [27] D. Bernardini, G. Rega, G. Litak, and A. Syta, *Proc. IMechE Part K: J. Multi-body Dynamics* 227, 17 (2013).
- [28] A. Wolf and J.B. Swift and H.L. Swinney, *Physica D* 16, 285, (1985).
- [29] H. Kantz, *Physics Letters A* 185, 77 (1994).
- [30] J. Aguirre, J.C. Vallejo, and M.A.F. Sanjuan, *Phys. Rev. E*, 64, 066208, (2001).
- [31] G. Litak, M. Coccolo, M.I. Friswell, S.F. Ali, S. Adhikari, A.W. Lees, and O. Bilgen, in Proc. of NSC 2012 4th IEEE International Conference on Nonlinear Science and Complexity August 6-11, 2012 Budapest, Hungary, 113-116, 2012.